# A multibeam opportunistic SAR system

Edison Cristofani, Virginie Kubica, Xavier Neyt
Royal Military Academy of Belgium, Electrical Engineering Dept.
Avenue de la Renaissance 30, B-1000 Brussels, Belgium
{Edison.Cristofani, Virginie.Kubica, Xavier.Neyt}@rma.ac.be

**Abstract**

SAR imaging has been historically performed using monostatic radar configurations where the transmitter and receiver shared the same location. Bistatic SAR is certainly not new. Cooperative bistatic SAR has been conducted either air-air, air-space and space-space [1]. Non-cooperative space-ground bistatic SAR as the one presented in this paper or in [2,3] present the advantages of being relatively cheap and able achieve a high revisit time by combining several satellites such as Envisat, ERS-2 or RADARSAT-2. From a tactical point, these systems are difficult to detect as they are passive.

The synchronization between the transmitter and the receiver is crucial in bistatic SAR systems. This is usually done physically, by having one antenna pointing towards the transmitter and another towards the scene. A particularity of the system described in this paper is that the receive antenna consists in a phased array and that phased array is used to separate the direct-path signal from the echo signal.

The spatial processing is described in a companion paper [4] while this paper concentrates on a description of the system, an analysis of the interferences present and present initial results.

## 1 Introduction

Synthetic Aperture Radar (SAR) imaging is typically conducted in monostatic radar systems. In monostatic systems both the transmitting and the receiving chains are at the same location, usually even sharing the same antenna. Monostatic SAR imaging system are thus inherently cooperative. Bistatic SAR imaging has gained popularity in the past years. Cooperative SAR imaging has been performed in multiple configurations: air-borne to air-borne [5], air-borne to space-borne [6,7], space-borne to space-borne [1,8]. and space-borne to ground [2,3].

Synchronization between the receiver and the transmitter is a key issue in bistatic radar and particularly in bistatic SAR. In non-cooperative system, a direct link between the transmitter and the receiver is excluded. Synchronization is thus usually based on the reception of the so-called direct path signal from the transmitter. This direct path signal is usually received using a dedicated antenna [2,3] and another antenna is used to receive echo signals from the scene.

The particularity of the system described in this paper is that a antenna array is used to receive both signals and the direct path signal is separated from the echo signal by spatial beamforming as described in [4]. This removes the need to manipulate an antenna dedicated to the reference signal at the price of a sensitive calibration [9].

Besides the absence of transmitter, a major advantage of passive bistatic SAR systems is that several transmitters of opportunity operating in the same frequency band can be considered as source. In C-band, the frequency band considered here, one has ENVISAT, ERS-2 and Radarsat-1/2. Considering several transmitters of opportunity increases the revisit time of the observed scene.

There are two main imaging scenarios illustrated in Figure 1 In the backscattering geometry, the illuminator and the receiving system are on the same side of the imaged scene. In

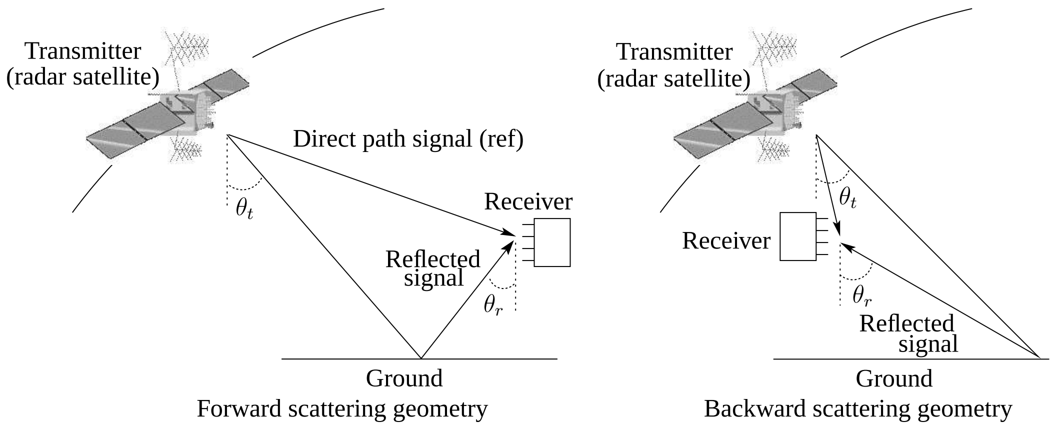


Figure 1: Possible imaging geometries. Left: back scattering geometry, Right: forward scattering geometry.

the forward scattering geometry, the imaged area is located between the illuminator and the receiver. The backscattering geometry provides the highest range resolution while the forward scattering geometry provides the highest signal thanks to a close-to-specular reflection of the signal on the imaged scene.

The paper is organized as follows. In Section 2, the system is described. Section 3 presents the received signals while early results are presented in Section 4. Finally, Section 5 concludes the paper.

# 2 System description

## 2.1 Bloc diagram

The bloc diagram of the receiving system is depicted in Figure 2. There are three main parts.

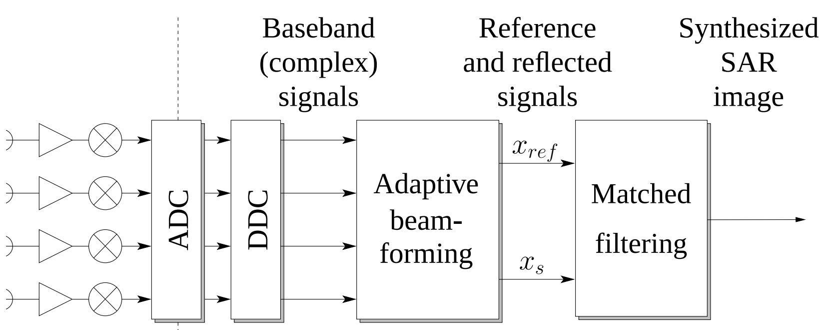


Figure 2: Bloc diagram of the passive radar system.

The first part consists in the receiver from the antenna till (digital) base-band signals. The separation between the direct-path signal and the echo signal including the synchronization is performed in the second part. And finally the image synthesis, combining range and azimuth compression is performed in the last part. These parts are further described in the sections below.

## 2.2 Reception system

A bloc-diagram of the reception system is depicted in Figure 3 and it is illustrated in Figure 4 (Left). It is a typically super-heterodyne receiver built using Minicircuits components.

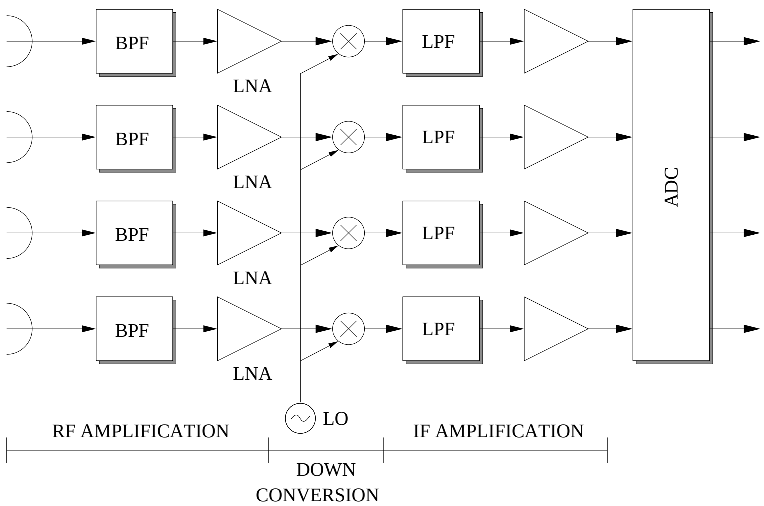


Figure 3: Block diagram of the reception part.

The antenna array at the receiver consists in 4 vertically polarized micro strip antennas as depicted in Figure 4 (Right). The main advantages of this type of antenna is that they are

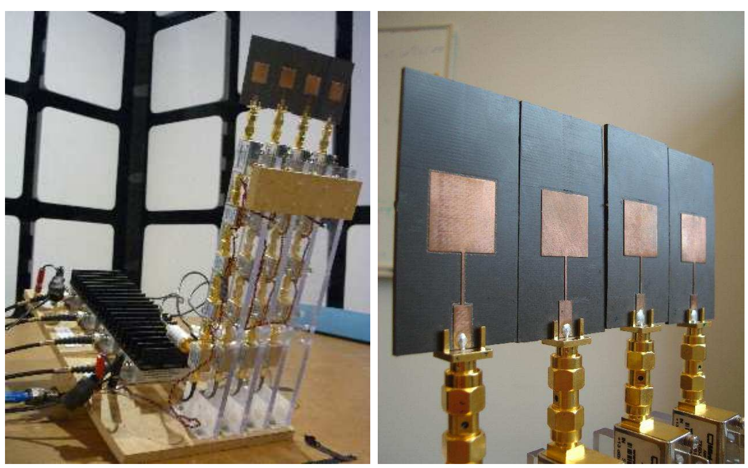

Figure 4: Receiving system (Left) and antenna array (Right).

relatively easy to manufacture and are relatively cheap. Size constraints were also a selection criteria since, to avoid grating lobes, the antennas need to be at most $\lambda/2$-spaced. The antennas where designed to operate at a resonance frequency of 5.4GHz and having a bandwidth sufficiently wide to cover the operating frequencies of ENVISAT, ERS-2 and Radarsat-1/2. The antennas where first simulated before being actually realized. The antennas where then characterized in an anechoic chamber. Figure 5 presents the theoretical antenna pattern and the measured antenna patterns in azimuth and in elevation.

The amplification is provided by a cascade of low noise amplifiers totaling a gain of 75 dB.

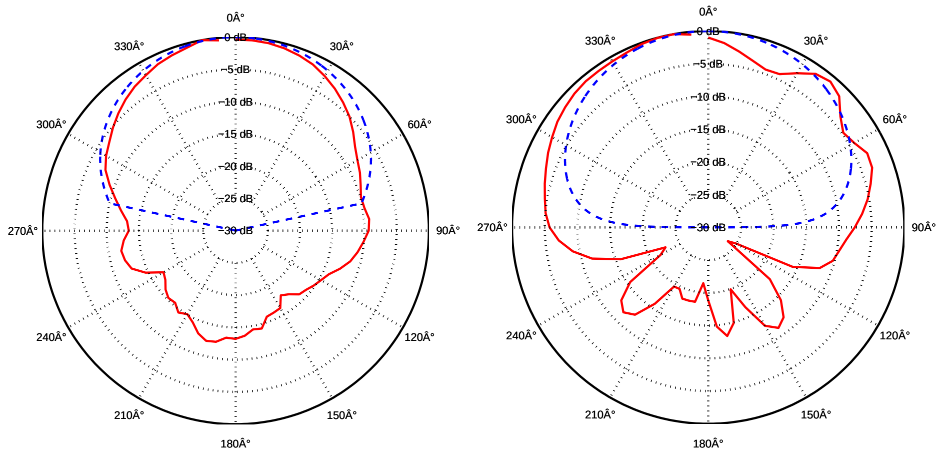


Figure 5: Antenna pattern of a single patch antenna in azimuth (Left) and in elevation (Right).

The downconversion is performed in two steps. In the first step, the received signal is down-converted to intermediate frequency (20 MHz) using a programmable local oscillator. By changing the frequency of the local oscillator, the receiver can be tuned to receive the signals from the different satellite. The intermediate frequency signal is then sampled at 50MS/s using a 16-bit A/D card (AlazarTech ATS660). It is finally digitally down-converted to base band thus providing the complex base band signal for further processing.

## 2.3 Signal separation

Signal separation consists in deriving the direct-path signal from the received mixture that contains both the direct path signal and the echo signal. There are two main goals: providing a direct path signal that will be used to perform range-compression and eliminating (or attenuating) the direct path signal present in the echo-signal. The latter is handled in a companion paper [4]. The former require a calibrated antenna array and a possible calibration procedure is described in [9]. The calibration of the antenna at elevation angles corresponding to the observed scene is still work in progress.

In the mean time, the direct-path signal is resynthesized. Since the considered illuminators of opportunity are all SAR satellites transmitting linear frequency-modulated (LFM) chirps, the shape of the transmitted signal is known. The only parameters that have to be estimated are the exact center frequency, the chirp length, the chirp rate and the initial phase. Indeed the center frequency depends on the drift between the local oscillator at the receiver and that at the transmitter. The chirp length and chirp rate depend on the particular mode in which the SAR instrument on board the spacecraft is operating at the time the spacecraft overflies the receiver. The initial phase is the phase difference of the local oscillatoris at the start of the transmission of the chirp and varies from chirp to chirp. It has of course to be estimated in order to recover a meaningful phase history in azimuth. The chirp rate, center frequency and initial phase are estimated by fitting the theoretical quadratic phase of a LFM chirp with the unwrapped phase of the direct signal pulse.

## 2.4 Image synthesis

Image synthesis is performed using matched filtering. First a compression in range is performed by matched filtering with the synthesized direct-path signal. In a second stage, the compression is performed in azimuth by matched filtering the range-compressed data along the along-track range-history curve.

The azimuth compression provides the resolution along the isorange curves. The isorange surfaces are ellipsoids with the transmitter and the receiver as focal points. If a locally flat earth surface is considered and if the receiver is located on the ground, the isorange curves on the ground are ellipses. In essence, the natural coordinate system of bistatic SAR imaging is thus approximately polar, centered at the receiver. This geometry fundamentally differs from the monostatic SAR geometry where, given the large range, the isorange are virtually parallel to the flight direction. In backscattering geometry, at larger ranges from the reciver, and for small opening angles, both geometries become equivalent.

# 3 Received signals

The receiving system was placed on the roof of a building in the center of Brussels, overlooking the neighboring area (Figure 6). The building being only slightly higher than the surrounding construction does not provide an optimum imaging geometry.

Figure 6: View towards the imaged area as seen from the receiver.

Typical received signals from the ENVISAT spacecraft are depicted in Figure 7. Burst

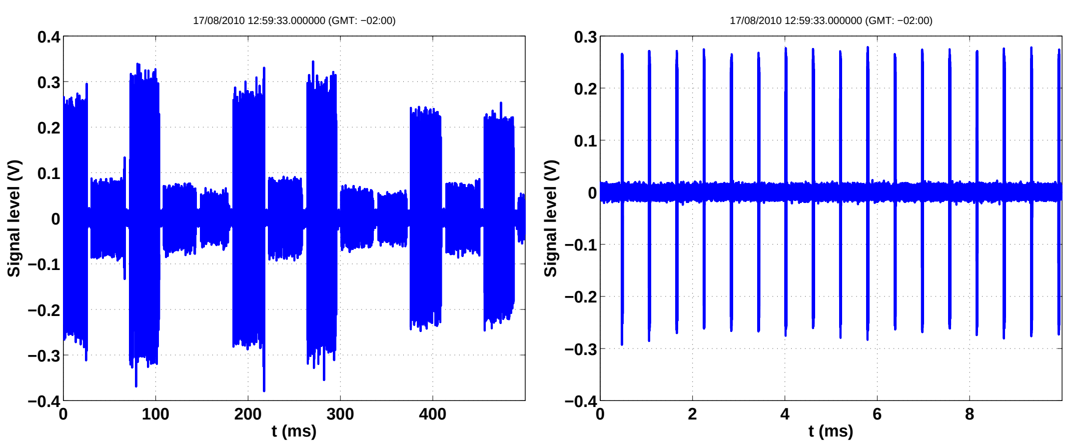


Figure 7: Acquired ENVISAT signal: Acquisition in ScanSAR mode (Left) and detailed pulse train (Left).

of chirps of varying amplitude are visible on the left part of Figure 7. This corresponds to the ScanSAR mode of ENVISAT where the beam is electronically steered in elevation to scan a large swath. Each burst corresponds to a particular scan at a different elevation. The amplitude variation is due to the fact that despite the changing pointing of the antenna beam and the receiver thus not being in the main lobe of the transmit antenna, signal is still received from the side lobes of the transmit antenna. Figure 7 (Right) presents a detailed view of one of the burst where the more classical pulses can be seen at regular intervals corresponding to the pulse repetition interval.

The received system is relatively sensitive to interferences. In particular, in the considered setup location (Brussels, Belgium) according to the radio spectrum regulation office (IBPT/BIPT), the frequency band below 5.35GHz may be used for Wireless Access Systems (WAS). These interferences possibly do less affect monostatic systems as the WAS would

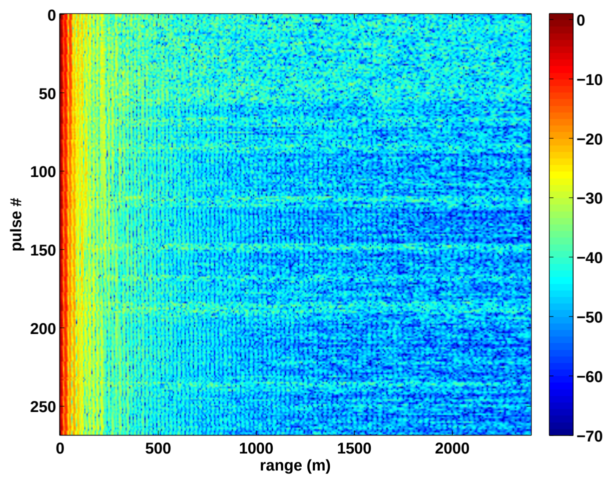


Figure 8: Range-compressed image with interferences (amplitude in dB).

only radiate in the horizontal direction, not upwards, towards the satellite. The bistatic receiver, being located on the ground resides within the main lobe of transmit antenna of those WAS. Figure 8 depicts a range-compressed image. On the left hand-side of the figure, the huge direct signal is to be seen and in the remainder of the picture, an interference pattern can be noticed.

# 4 Early results

Figure 9 presents a synthesized image in ground range. The blue circles on that graph are drawn at 400m ground range distance increments from the receiver. The huge point target corresponds to the receiver. That strong signal is actually due to the range and azimuth compression of the direct-path signal. This early result is rather disappointing. In order to assess whether what is seen is actual data or noise, the distribution of the measured backscatter is evaluated in two different areas. The first area (the blue boxes in Figure 9 (Left)) is located within the main beam of the receive antenna and is actually expected to contain data. For the test to be relevant, the area where range sidelobes of the direct path signal are expected should be excluded hence the gap between the two blue boxes. The second area (the red box in Figure 9 (Left)) is located in the sidelobes of the receive antenna and should thus contain less signal. The distribution of the measured backscatter is depicted in Figure 9 (Right). And, as expected, the backscatter is higher in the main beam of the antenna.

Our analysis of the disappointing results is that first the azimuth resolution is limited due to a too short acquisition and second the observed scene is possibly too complex. Further

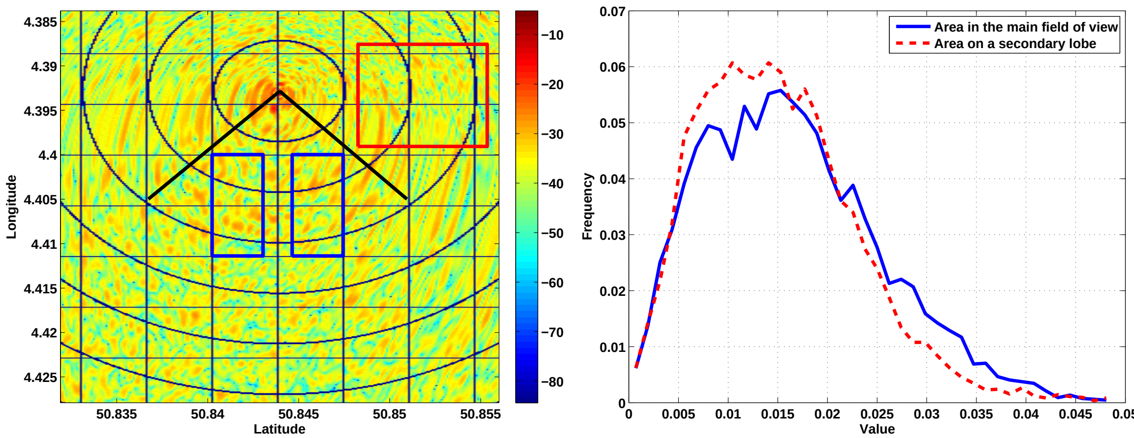


Figure 9: Range-compressed image with interferences (amplitude in dB).

steps include moving the receiver to a more appropriate location with an easy to interpret scene.

# 5 Conclusions and future work

This paper presents a passive opportunistic SAR system using SAR satellites operating in C-band as illuminators. The challenge of the phase synchronization between the transmitter and the receiver was discussed. Image synthesis is performed in two steps: signal separation, providing a reference signal from which phase synchronization information is extracted followed by a compression in range and in azimuth. First images where presented and an assessment of signal presence was done.

Besides the relocation of the receiver and the acquisition of longer signals, we intend to put a point target out in the scene in order to help characterize the performance of the system in terms of resolution and SNR. Indeed “natural” point targets seems to be relatively rare in bistatic radars. A comparison of the obtained bistatic image with the corresponding monostatic image will also be performed.

# References

[1] G. Krieger, I. Hajnsek, K. Papathanassiou, M. Younis, and A. Moreira, “Interferometric synthetic aperture radar (SAR) missions employing formation flying,” *Proceedings of the IEEE*, vol. 98, pp. 816–843, May 2010.

[2] J. Sanz-Marcos, P. Lopez-Dekker, J. J. Mallorqui, A. Aguasca, and P. Prats, “SABRINA: A SAR bistatic receiver for interferometric applications,” *IEEE Geoscience and Remote Sensing Letters*, vol. 4, Apr. 2007.

[3] A. Broquetas, P. Lopez-Dekker, J. J. Mallorqui, A. Aguasca, M. Fortes, J. C. Merlano, and S. Duque, “SABRINA-X: Bistatic SAR receiver for TerraSAR-X,” in *8th European Conference on Synthetic Aperture Radar*, (Aachen, Germany), 2010.

[4] V. Kubica, E. Cristofani, and X. Neyt, “Strategies for mitigating the strong direct path signal in passive bistatic SAR imaging,” in *Proc. of the first joint WIC/IEEE SP Symposium on Information Theory and Signal Processing in the Benelux*, (Brussels, Belgium), May 2011.

[5] P. Dubois-Fernandez, H. Cantalloube, B. Vaizan, G. Krieger, R. Horn, M. Wendler, and V. Giroux, “ONERA-DLR bistatic SAR campaign: planning, data acquistiton, and first analysis of bistatic scattering behaviour of natural and urban targets,” *IEEE Proceedings – Radar, Sonar and Navigation*, vol. 153, pp. 214–223, June 2006.

[6] M. Rodriguez-Cassola, S. Baumgartner, G. Krieger, and A. Moreira, “Bistatic TerraSAR-X/F-SAR spaceborne-airborne SAR experiment: Description, data processing, and results,” *IEEE Trans. on Geoscience and Remote Sensing*, vol. 48, pp. 781–794, Feb. 2010.

[7] I. Walterscheid, T. Espeter, A. Brenner, J. Klare, J. Ender, H. Nies, R. Wang, and O. Loffeld, “Bistatic SAR experiments with PAMIR and TerraSAR-X setup, processing, and image results,” *IEEE Trans. on Geoscience and Remote Sensing*, vol. 48, pp. 3268 – 3279, Aug. 2010.

[8] M. Eineder, G. Krieger, and A. Roth, “First data acquisition and processing concepts for the TanDEM-X mission,” in *Proceedings of ISPRS (International Society for Photogrammetry and Remote Sensing) Commission I Symposium*, (Paris, France), 2006.

[9] V. Kubica, R. Hock, E. Cristofani, and X. Neyt, “Strategies for the calibration of an array of patch antennas in passive bistatic SAR imaging,” in *Proc. of the IEEE Radar conference*, (Kansas City, MI), May 2011.